ACTA NEUROBIOLOGIAE EXPERIMENTALIS

Research Paper Acta Neurobiol Exp 2014, 74: 1–14

Aromatase and estrogen receptor beta expression in the rat olfactory bulb: Neuroestrogen action in the first relay station of the olfactory pathway?

Zsófia Hoyk[1], Eszter Csákvári[1], Andrea Gyenes[1], László Siklós[1], Nobuhiro Harada[2] and Árpád Párducz[1]*

[1]Institute of Biophysics, Biological Research Centre, Szeged, Hungary, *Email: parducz.arpad@brc.mta.hu; [2]Department of Biochemistry, School of Medicine, Fujita Health University, Toyoake, Aichi, Japan

The expression pattern of aromatase (ARO), the enzyme converting androgens to estrogens, was analyzed in the olfactory bulb of adult male rats and was compared with the distribution of estrogen receptor β (ERβ), the main estrogen receptor isoform expressed in this brain region. A strong ARO immunolabeling obtained with a specificity tested antibody was observed in juxtaglomerular neurons of the glomerular layer and a weaker immunoreaction was detected in the mitral cell layer of the main olfactory bulb, while the granule cell layer of the main olfactory bulb as well as all layers in the accessory olfactory bulb showed faint immunolabeling. Fluorescence double labeling experiments revealed that ARO detected in juxtaglomerular neurons of the main olfactory bulb colocalized with tyrosine hydroxylase (TH) and glutamic acid decarboxylase 67 (GAD67), while no colocalization between ARO and the calcium binding proteins calretinin (CR) and calbindin (CB) was observed. Furthermore, the TH immunoreactive neurons expressed metabotropic glutamate receptor 1 (mGluR1) too. ERβ immunoreactivity, in contrast to ARO, was detected in all layers of both the main and accessory olfactory bulb. In the glomerular layer of the main olfactory bulb it was expressed in TH and GAD67 containing juxtaglomerular neurons, and it colocalized with CR, CB and even with glial fibrillary acidic protein too. Our morphological findings suggest that ARO expression is a novel feature of dopaminergic/GABAergic juxtaglomerular neurons in the adult rat main olfactory bulb, and raise the possibility that ARO activity may change in function of olfactory input *via* mGluR1. *In situ* estrogen production in the olfactory bulb in turn may modulate interglomerular circuits through ERβ.

Key words: estradiol receptor β, tyrosine hydroxylase, glutamic acid decarboxylase 67, metabotropic glutamate receptor 1, calcium binding protein

INTRODUCTION

Since the discovery of brain aromatase (ARO) (Naftolin et al. 1971), the enzyme which is responsible for the conversion of androgens to estrogens (Stoffel-Wagner 2001), extensive research has been dealing with its expression pattern and activity, as well as with the role played by estradiol formed locally in the brain (Lephart 1996, Garcia-Segura 2008, Roselli et al. 2009). ARO activity was first detected in brain areas involved in reproductive functions and behaviors, such as the hypothalamus and limbic system of monkeys and rats (Flores et al. 1973, Roselli et al. 1985), but later it was observed in several other regions as well (MacLusky et al. 1994). The distribution map of the enzyme in the central nervous system was refined with immunohistochemical methods, revealing ARO immunoreactive neurons in all regions where ARO activity had been measured in rats and mice (Jakab et al. 1993, Shinoda et al. 1994, Foidart et al. 1995). In addition, ARO expression was found in locations not previously recognized to contain this enzyme such as the rat olfactory tract and piriform cortex (Sanghera et al. 1991), hippocampus of rats, monkeys and humans (Hojo et al. 2004, Yague et al. 2008, 2010), human cerebral cortex and other areas (Azcoitia et al. 2011a). Furthermore, ARO immunoreactivity was examined at the subcellular level too, and was observed in soma-

Correspondence should be addressed to Á. Párducz
Email: parducz.arpad@brc.mta.hu

Received 06 September 2013, accepted 26 November 2013

ta, dendrites and axon terminals of hypothalamic and limbic cell groups of various species (Naftolin et al. 1996).

Estradiol synthesized locally in the brain by the enzyme ARO is involved not only in reproductive behavior, but in several other functions, including neuroprotection after injury (Mirzatoni et al. 2010, Azcoitia et al. 2011b), mood and cognition (Garcia-Segura 2008), neurogenesis (Abrous et al. 2005), and synaptic plasticity (Fester et al. 2011), too. Furthermore, Jeong and coauthors (2011a) have suggested a common feature of information processing in sensory systems, at least in the auditory and the visual system, where brain-generated estradiol might play a role. Other sensory systems, such as the olfactory system, have not been examined in this respect, despite existing evidence on the involvement of olfactory pathway related ARO expression and/or activity in reproductive behavior. This link between ARO expression in the olfactory pathway and reproductive behavior is documented in various species, including fish, snakes and mice: ARO expression in the olfactory bulb varies with social status of male and with reproductive condition of female fish (Maruska and Fernald 2010), ARO activity is reported to show seasonal differences in the olfactory region of snakes (Krohmer et al. 2010) and fish (González and Piferrer 2003), ARO acting in central brain regions of olfaction is involved in reproductive behavior in female mice (Pierman et al. 2008), and brain-derived estradiol plays an activational role in coital behavior of male mice (Bakker et al. 2004).

Immunohistochemical studies carried out in the first relay station of the olfactory pathway, i.e. the olfactory bulb (OB) described ARO immunoreactivity in cell bodies of mitral cells and in processes in the glomerular layer (GL) of the main olfactory bulb (MOB), and in processes and cell bodies of the granule cell layer (GCL) in the accessory olfactory bulb (AOB) in the rat during development (Horvath and Wikler 1999). In the adult, the human placental antigen X-P_2, an antigen complex associated with cytochrome P-450 of ARO, was reported to be present in mitral and in internal, middle and external tufted cells of the MOB, while no immunostained cells were observed in the AOB (Shinoda et al. 1990), and ARO was directly detected in the canine MOB in mitral and granule cells (Karahan et al. 2008). However, no detailed morphological analysis have been carried out so far aiming to examine the capacity of the olfactory bulb to produce estradiol and respond to it, which would provide support for a possible involvement of ARO, and, consequently, locally synthesized estradiol in olfactory information processing.

The aim of the present study was to link production and sensitivity to estradiol in the adult male rat OB by analyzing the ARO immunoreactivity pattern, comparing it with the distribution of estrogen receptor (ER) β, the predominantly expressed ER isoform in the OB (Shughrue et al. 1997, Guo et al. 2001, Mitra et al. 2003), and characterizing the neurochemical properties of ARO and ERβ containing cells of this brain region.

Special attention was paid to the GL, where olfactory information is transmitted to principal output neurons (Shipley and Ennis 1996), and more specifically to the possible colocalization of ARO and/or ERβ with the main neurotransmitters of type I periglomerular neurons, γ-amino-butiric acid and dopamine, and with the calcium binding proteins calbindin D-28K (CB) and calretinin (CR), characteristics of type II periglomerular cells (Kosaka et al. 1995, 1997, 1998, Crespo et al. 2003).

METHODS

Animals

In the experiments two-month-old male Wistar rats were used. The animals were raised and maintained on a dark-light cycle with lights on at 07:00 AM and off at 07:00 PM in standard laboratory conditions, with tap water and regular rat chow available *ad libitum*. All efforts were made to minimize the number of animals used and their suffering. The principles of laboratory animal care (National Institutes of Health publication no. 8523), the protocol for animal care approved by the Hungarian Health Committee (1998) and the European Communities Council Directive (86/609/EEC) were followed. The study was approved by the Animal Use and Care Committee of the Biological Research Centre, Szeged, Hungary. Altogether 30 animals were sacrificed: 10 rats were used for single labeling immunohistochemistry and 20 animals were used for fluorescence double labeling experiments.

Antibody specificity testing

Two key antibodies were used in our immunohistochemical experiments: (1) anti-ARO polyclonal rabbit antibody (Santa Cruz Biotechnology Inc., sc-30086), which recognizes an epitope that corresponds to amino acids 209-503 mapping at the C-terminus of CYP19 of human origin, and (2) anti-ERβ rabbit polyclonal antibody recognizing an epitope corresponding to amino acids 1-150 of ERβ of human origin (Santa Cruz Biotechnology Inc., sc-8974). The specificity of the anti-ERβ antibody is accepted in over 90 research articles reporting data obtained with this antibody. The anti-ARO antibody, however, does not have many citations. Since the specificity of the ARO immunolabeling was also fundamental in our experiments, we performed two series of immunostainings in order to examine the reliability of this antibody. In one series of immunohistochemical experiments the staining pattern of this antibody was compared with that of another another ARO rabbit polyclonal antibody, a generous gift of Dr. L.M. Garcia-Segura, generated from a 15-amino acid peptide corresponding to residues 488-502 of mouse ARO, a region homologous to human and monkey ARO (Garcia-Segura et al. 1999, Yague et al. 2006). The two ARO antibodies (sc-30086 in a dilution of 1:500 and the antibody provided by Dr. L.M. Garcia-Segura in a dilution of 1:2 000) gave the same staining pattern. In another series of specificity testing the same immunohistochemical staining procedure was performed on olfactory bulb sagittal sections derived from wild type and ARO knockout mice. The sc-30086 ARO antibody gave no immunolabeling on sections of the ARO knockout mouse, while the olfactory bulb of the wild type mouse showed the same characteristic staining pattern observed already in our first series of specificity testing, with a strong immunolabel present in juxtaglomerular neurons (Fig. 1).

Single labeling immunohistochemistry

Animals were deeply anaesthetized with 2% (w/v) tribromoethanol (Aldrich) (1 mL/kg body weight), then they were perfused intracardially with 0.9% sodium chloride (Sigma) dissolved in 0.01 M phosphate buffer, pH 7.4 (PB), followed by 4% (w/v) paraformaldehyde (Sigma) in 0.1 M PB, pH 7.4. After perfusion the OBs were dissected out and postfixed for 4 h in the same fixative. Following fixation the OBs were washed in 0.1 M PB, pH 7.4, and cryoprotected in 30% (w/v) sucrose (Sigma) until saturation. Then, sagittal sections of the OB containing the AOB with nominal thickness of 30 µm were cut on a cryostat (Floorstanding Cryostat MNT; Slee, Mainz, Germany), collected in 0.1 M PB, pH 7.4 containing 0.01% sodium azide (Fluka AG) (w/v) and were stored at 4°C.

The immunohistochemical stainings were carried out using the avidin-biotin-peroxidase method (Hsu et al. 1981). Free floating sections were rinsed (3×10 min) in a buffer composed of 0.1 M PB, pH 7.4, 0.9% (w/v) sodium chloride (Sigma) and 0.3% (w/v) bovine serum albumin (PBS-BSA). Non-specific immunoreactivity was blocked by incubating the sections in 5% (v/v) normal goat serum (Sigma) in PBS-BSA for 1 h at room temperature. Then, sections were incubated in the following primary antibodies: (1) anti-ARO polyclonal rabbit antibody (Santa Cruz Biotechnology Inc., sc-30086, 1:500) and (2) anti-ERβ rabbit polyclonal antibody (Santa Cruz Biotechnology Inc., sc-8974, 1:500). All primary antibodies were diluted in PBS-BSA and

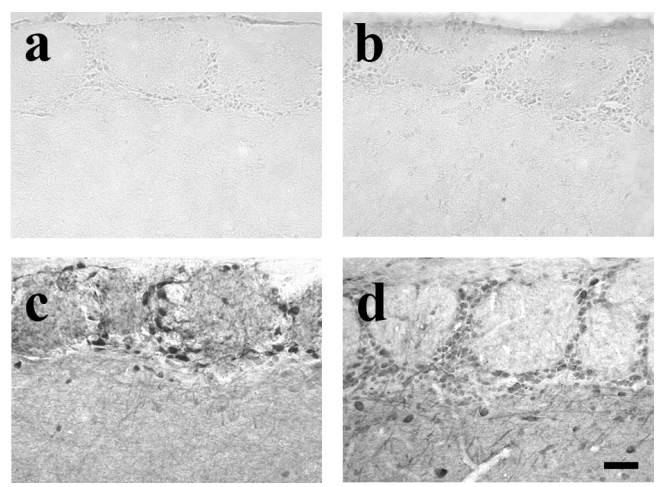

Fig. 1. ARO immunoreactivity pattern in the GL of the MOB. A cryostat section from the MOB of ARO knockout mouse on which no immunostaining was performed is shown in panel (a), while the section of the MOB of ARO knockout mouse in panel (b) underwent an immunohistochemical procedure using the sc-30086 ARO antibody (1:500). Note the lack of immunolabeling. The same immunohistochemical procedure using the sc-30086 ARO antibody (1:500) was applied to the section of the MOB from a wild type mouse shown in panel (c). A strong, characteristic immunostaining is present in the juxtaglomerular cells surrounding glomeruli. Panel (d) demonstrates the same immunoreactivity pattern obtained with the ARO antibody (1:2 000) donated by Dr. LM. Garcia-Segura. Scale bar is 50 µm.

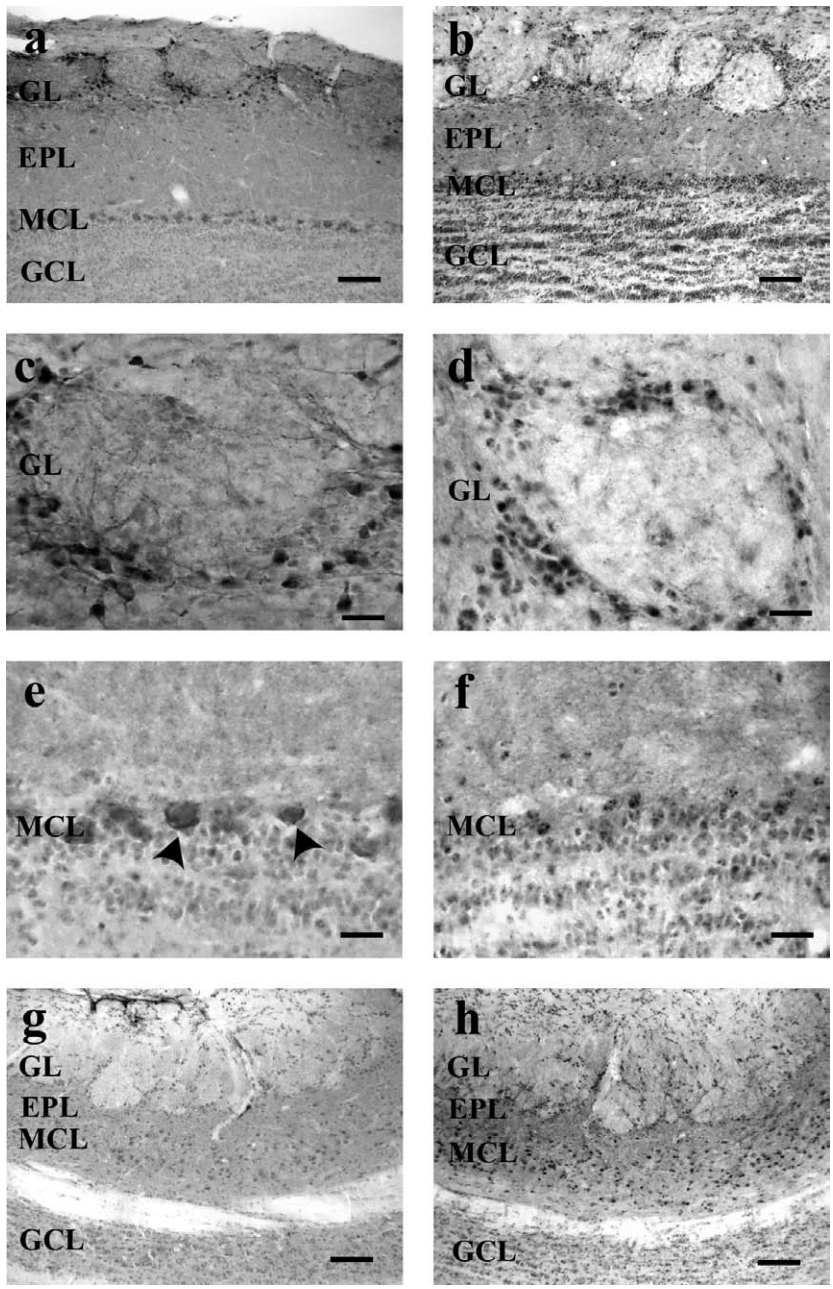

Fig. 2. Distribution pattern of ARO (a, c, e, g) and ERβ (b, d, f, g) immunoreactivity in the adult male rat OB. The ARO antibody labels most intensively the GL, gives a moderate staining in the MCL, stains weakly the GCL in the MOB (a), and shows a faint immunoreactivity in the whole AOB (g). ARO immunolabel is detected in somata and cellular processes, delineating the morphology of neurons. In the GL small juxtaglomerular neurons are highlighted by the ARO immunoreactivity product, localized mainly in the cytoplasm, and thin neuronal processes entering and delineating the glomerulus are also labeled (c). The ARO immunostaining in mitral/tufted cells is weaker then in juxtaglomerular cells, but it shows the same pattern: it is localized in the thin cytoplasmic compartment, surrounding the nuclei, as indicated with arrowheads (e). ERβ immunoreactivity is distributed throughout the MOB and AOB (b, d, f, g). It is present predominantly in cellular nuclei in all layers, but a weaker membrane staining can also be observed, especially in the EPL and in some processes entering the glomeruli. The ERβ immunolabel in cellular nuclei displays a characteristic "speckled" pattern, as it is seen in small juxtaglomerular cells (d) and in large mitral/tufted cells, too (f). The glomerulus seen in (c) and (d) and the mitral/tufted cells seen in (e) and (f) are higher magnifications of a glomerulus and some mitral/tufted cells in (a) and (b), respectively. Scale bars are: 100 μm (a, b, g, h) and 50 μm (c, d, e, f).

all incubations were carried out for 48 h at 4°C. Following incubation with the primary antibodies sections were rinsed in PBS-BSA (3×10 min) and incubated with biotinylated donkey anti-rabbit IgG (Jackson ImmunoResearch Europe Ltd., 1:1 000) for 2 h at room temperature. Then, sections were washed in PBS-BSA (3×10 min) and incubated in Vectastain Elite ABC reagent (Vector, 1:250) for 1 h at room temperature. Sections were rinsed in 0.1 M PB, then the reaction product was visualized by incubating the sections in 0.042% (w/v) 3,3'-diaminobenzidine (DAB, Sigma) and 0.002% (v/v) hydrogen peroxide (Sigma) in 0.1 M PB, pH 7.4 for 5 min. The immunostained sections were mounted on slides, dehydrated in an ascending series of alcohol, coverslipped with Entellan (Merck) and analyzed with a Nikon Eclipse 80i upright microscope (Nikon Instruments Europe B.V., Amstelven, The Netherlands) equipped with a Z-focus module (Model 805 RFAERGO1, Conix Research, Springfield, USA) and a 5.1 megapixel CCD camera (Micropublisher 5.0 RTV, Adept Turnkey Pty Ltd, Perth, Australia), attached to a HP Workstation XW4600 personal computer.

For high resolution imaging, a series of images at different focus settings were acquired at selected positions of the sections with the Scope-Pro Plus module of the Image-Pro Plus image analysis program (version 7.0, Media Cybernetics, Bethesda, USA) using either the 40× or the 100× objective of the microscope. First, with the aid of the Z-focus module of the microscope, the local section thickness was measured which, as a consequence of the (unknown) difference between the nominal thickness value of the cryostat and the true section thickness, furthermore due to the shrinkage of the sections during dehydration, finally, proved to be 10 µm, in average. Next, following a white balance correction, starting at the bottom of the section, a systematic set of 20 images was collected at 500 nm distances in the Z-direction with the camera setting of 2 560×1 920 pixels at 24 bit color. After conversion to gray scale, this set of images was used to generate a single best focus composite image by means of the extended depth of field operation of the Image-Pro Plus program with the maximum local contrast and the normalized illumination parameters switched on.

Double-immunofluorescence histochemistry

Free floating sagittal sections were rinsed in PBS-BSA for 3×10 min, then incubated in 5% (v/v) normal goat serum (Sigma) in PBS-BSA for 1 h at room temperature to block non-specific immunoreactivity. In the first series of double labeling experiments ARO was colocalized either with tyrosine hydroxylase (TH), glutamic acid decarboxylase 67 (GAD67), CB or CR. Cocktails of primary antibodies were prepared in PBS-BSA at dilutions as follows: anti-ARO rabbit polyclonal antibody (Santa Cruz Biotechnology Inc., sc-30086, 1:100) and either (1) mouse anti-TH (Millipore, MAB318, 1:1 000), or (2) mouse anti-GAD 67 (Millipore, MAB5406, 1:100), or (3) mouse anti-CB (Swant, no. 300,1:5 000), or (4) 1:100 mouse anti-CR, a generous gift of Dr. M.A. Arevalo, which was raised in mice according to the method of Ou and colleagues (1993) using human recombinant CR (Swant) as antigen and purified by fast protein liquid chromatography. This polyclonal ascites fluid antibody recognizes a unique band of 29 kD in homogenates from rat brain, and in our OB sections at a dilution of 1:100 it shows the same staining pattern as the rabbit polyclonal anti-CR (Chemicon, AB5054) at a dilution of 1:10 000. Another series of sections was incubated in a cocktail of antibodies containing mouse anti-TH (Millipore, MAB318, 1:1 000) and rabbit anti-metabotropic glutamate receptor 1 (mGluR1) (Abcam, ab82211, 1:250), which detects a single band of approximately 110 kDa (predicted molecular weight 133 kDa) according to the manufacturer's data sheet.

In the second series of double labeling studies sections were incubated with cocktails of antibodies containing anti-ERβ rabbit polyclonal antibody (Santa Cruz Biotechnology Inc., sc-8974, 1:100) and either mouse anti-glial fibrillary acidic protein (GFAP) (Sigma, G3893, 1:30 000), or one of the same antibodies that were used in ARO double stainings, namely (1) mouse anti-TH (Millipore, MAB318, 1:1 000), (2) mouse anti-GAD 67 (Millipore, MAB5406, 1:100), (3) mouse anti-CB (Swant, no. 300, 1:5 000) and (4) mouse anti-CR, a generous gift of Dr. M.A. Arevalo (at a dilution of 1:100). All primary antibodies were diluted in PBS-BSA and all incubations were carried out for 48 h at 4°C. Then, sections were carefully rinsed in PBS-BSA (3×10 min) and they were incubated with the following secondary antibodies: DyLight™549-conjugated goat anti-rabbit IgG (Jackson ImmunoResearch Ltd., 1:100) and DyLight™488- conjugated goat anti-mouse IgG (Jackson ImmunoResearch Ltd., 1:100) for 2 h at room temperature. Counterstaining was performed in 300 nM 4'6-diamino-2-phenylindole

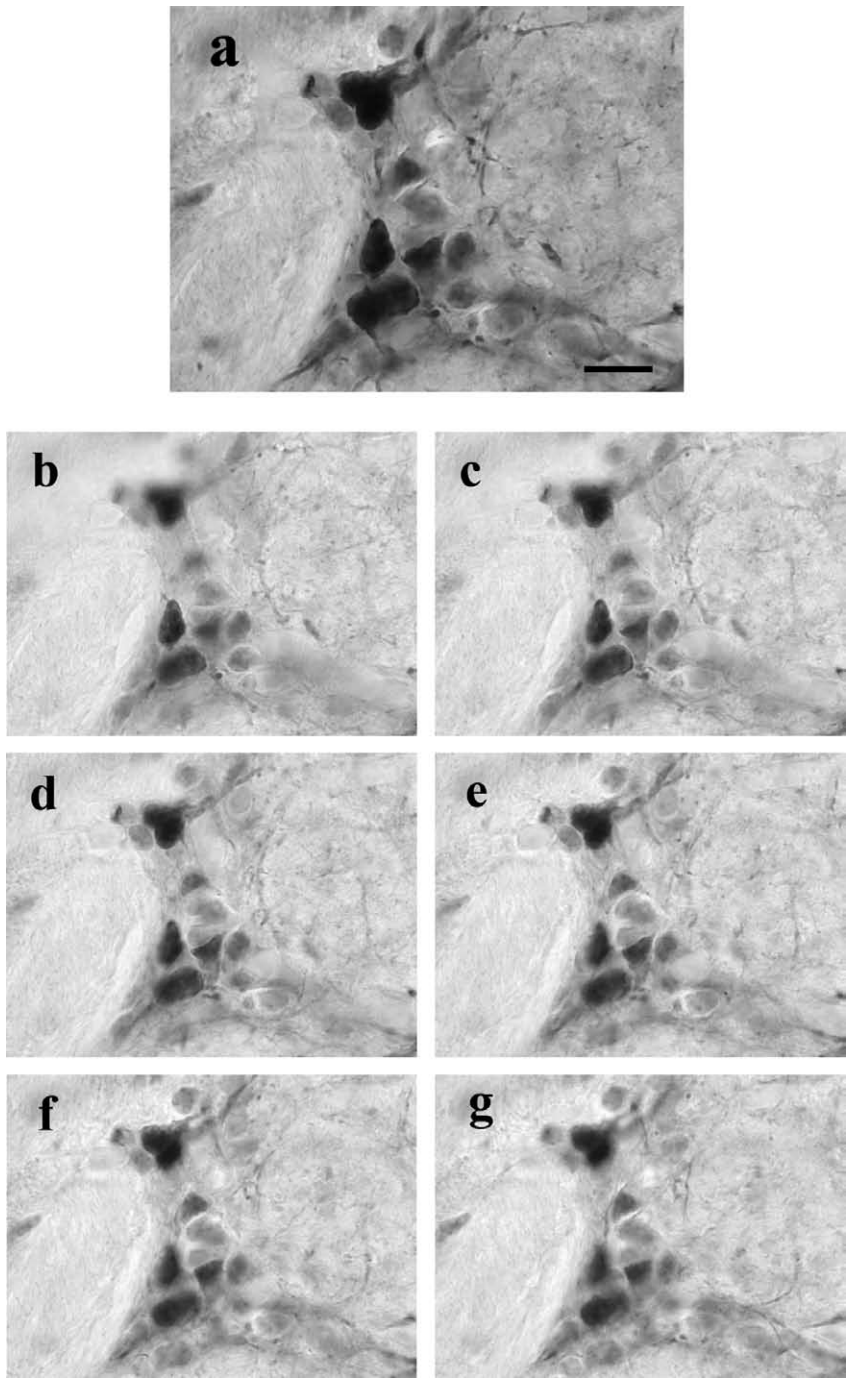

Fig. 3. Distribution pattern of ARO immunoreactivity in the periglomerular region of adult male rat OB. The ARO antibody labels most intensively the cytoplasm of the somata and cellular processes of the juxtaglomerular cells, delineating the morphology of neurons. Transmission light microscopic image at high resolution (a) was obtained by focusing through the section at 500 nm steps and generating a single best focus composite image by means of the extended depth of field operation of the Image-Pro Plus program with the maximum local contrast and the normalized illumination parameters switched on. A series of images obtained at 500 nm focal distances (b–g) suggests that the ARO immunoreactivity product is not distributed evenly in the cytoplasm, but rather in thin cytoplasmic compartments located in different parts of the soma, sometimes very close to the nuclei. Even a nuclear staining might also be perceived virtually due to overprojection of staining of neighboring cells with characteristic size less than the thickness of the section (The maximal diameter of periglomerular cells is in the range of 5–10 μm). Scale bar is 10 μm.

(DAPI) (Sigma) in 0.1 M PB, pH 7.4 for 5 min. Sections were mounted on glass slides, coverslipped with Confocal-Matrix® (Micro-Tech-Lab) and examined with a confocal laser scanning microscope (Olympus Fluoview FV1000, Olympus Life Science Europa GmbH, Hamburg, Germany). Microscope configuration was the following: objective lens: UPLSAPO 60× (oil, numeric aperture: 1.35); sampling speed: 10 μs/pixel; scanning mode: sequential unidirectional; excitation: 405 nm (DAPI), 488 nm (DyLight 488) and 543 nm (DyLight 549).

RESULTS

ARO and ERβ expression pattern

Single immunolabeling studies analyzing the expression pattern of ARO in the adult male rat OB showed DAB immunoreactivity in the cytoplasm of somata and cellular processes revealing the morphology of neurons. Labeled cells were detected in every layer of the MOB and the intensity of immunostaining differed according to neuron types: small granule cells displayed a faint immunolabel, large mitral and tufted cells were moderately labeled, and several neurons in the GL were characterized by a strong immunoreaction (Fig. 2a). Neurons in the GL, i.e. juxtaglomerular cells, had small somata, some of their processes entered the glomeruli and many of them passed along glomerular borders, partially "embracing" glomeruli. In most of ARO immunoreactive juxtaglomerular neurons the immunolabel was detected in the cytoplasm and neuronal processes, and in some cells a presumably virtual nuclear staining can be perceived (Fig. 2c). Mitral cells displayed a less intensive staining compared to juxtaglomerular neurons. The DAB immunoreactivity product was localized in a thin cytoplasmic layer, surrounding the nuclei (Fig. 2e). Interestingly, a clear difference was detected in ARO expression when comparing the immunostaining of the MOB with that of the AOB within the same section. The AOB, in contrast to the MOB, showed a uniform, faint labeling in every layer (Fig. 2g).

In order to further characterize the ARO immunostaining, high resolution images were obtained from labeled juxtaglomerular cells of the MOB displaying the strongest immunoreaction. The exact distribution of the DAB reaction product could be examined in these cells only at high resolution and magnification, due to their small (ca. 5–10 μm) soma size and due to the partial overlapping of these cells in the section. High resolution images revealed that the ARO immunoreactivity product was characteristically localized in distinct compartments of the thin cytoplasm (Fig. 3), resembling the type of labeling seen in MOB mitral cells (Fig. 2e). Some neighboring neurons with characteristic size less than the thickness of the section may overproject their immunolabel to each other, producing the perception of a possible nuclear staining.

Having examined the ARO immunolabeling pattern in the OB, we compared it with the distribution of ERβ immunoreactivity. In the MOB, the antibody recognizing ERβ gave a strong labeling in many nuclei of the mitral cell layer (MCL) and GL, in cells scattered in the external plexiform layer (EPL), and in some nuclei in the GCL. Furthermore, a weaker immunostaining was observed on cellular processes in the EPL and on some processes entering the glomeruli (Fig. 2b). The ERβ immunoreactivity product showed a characteristic "speckled" pattern in the nuclei of all labeled cells. This pattern is best seen in larger cells, like mitral cells (Fig. 2f), but it can be perceived in small juxtaglomerular cells, too (Fig. 2d). In contrast to ARO immunostaining, ERβ immunolabeling is observed in the same pattern and distribution in the AOB as in the MOB (Fig. 2h). Thus, ERβ expression partially overlaps with ARO immunoreactivity pattern, but in general it is characterized by a more widespread distribution in the whole OB.

Neurochemical characterization of ARO expressing juxtaglomerular cells

Although the juxtaglomerular cells of the MOB in rodents are well characterized regarding their anatomical and neurochemical properties (Kosaka et al. 1995, 1997, 1998, Toida et al. 2000, Crespo et al. 2003, Kosaka and Kosaka 2005, 2008, 2011, Parrish-Aungst et al. 2007), ARO immunoreactivity has not been described before in these neurons. Given the heterogeneity of juxtaglomerular neurons, a series of colocalization studies was performed in order to find out the chemotype of ARO expressing cells in the GL.

The morphology of ARO immunolabeled cells characterized by small somata with dendrites entering and passing along glomeruli resembled dopaminergic peri-

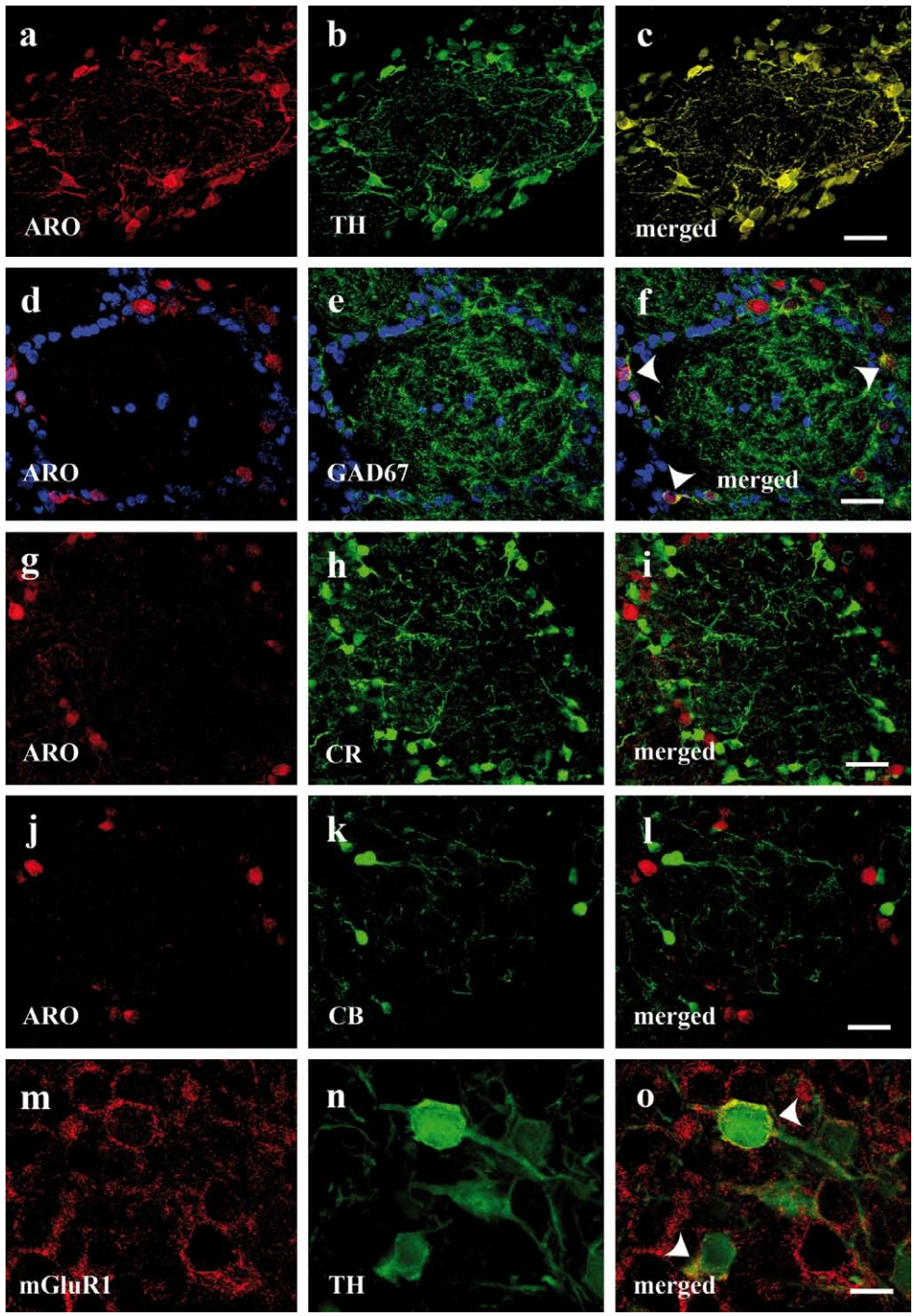

Fig. 4. Confocal images [10-µm stack for (a–c), single slices for (d–o)] of double fluorescences in the GL of the MOB to analyse the colocalization of ARO with TH (a–c), GAD67 (d-f), CR (g–i), CB (j-l) and the colocalization of TH with mGluR1 (m–o). ARO+ cells are displayed in red (a, d, g, j), TH+ (b), GAD67+ (e), CR+ (h) and CB+ neurons (k) are seen in green. Sections immunolabeled with ARO and GAD67 were counterstained with DAPI (blue). Overlays of images show a complete colocalization of ARO with TH (c). All ARO+ neurons contained GAD67, but GAD67+ neurons were more numerous than ARO+ cells. Arrowheads point to ARO/GAD67 double labeled cells(f). ARO never colocalized neither with CR (i), nor with CB (l). TH immunoreactive neurons (n, displayed in green) expressed mGluR1 (m, labeled in red) on their cellular membranes, as shown in the merged image. Arrowheads indicate mGluR1 expressing TH immunolabeled neurons (o). Scale bars are: 30 µm (a–l), 10 µm (m–o).

glomerular neurons, thus first we performed a double immunofluorescence staining with ARO and TH antibodies. Both ARO and TH immunolabeling was observed in the cytoplasm, filling somata and neuronal processes as well. The pattern and intensity of ARO and TH immunostaining was the same in all animals studied. A thorough examination of the distribution of immunoreactivities with the confocal microscope revealed that all ARO immunolabeled neurons were immunoreactive also for TH in the GL of the MOB in every section. It suggests a total colocalization of ARO with TH in the juxtaglomerular neurons of the MOB (Fig. 4a, b, c).

In order to get a more precise neurochemical characterization of these ARO expressing neurons that proved to be dopaminergic, we carried out an analysis of colocalization of ARO and GAD67, since the dopaminergic juxtaglomerular neurons are known to express the 67 kD isoform of the GABA synthesizing enzyme (Kiyokage et al. 2010). The ARO immunolabel was homogeneously distributed in the cytoplasm of juxtaglomerular neurons, just as in double labeling experiments with the TH antibody. The GAD67 antibody labeled a larger number of cells than the ARO antibody, giving a patchwork-like signal that filled also somata and neuronal processes, developing a dense network inside the glomeruli. We found that ARO containing neurons formed a subpopulation of GAD67 immunoreactive juxtaglomerular cells: all ARO immunostained neurons were labeled with the GAD67 antibody as well (Fig. 4d, e, f). This result is in accordance with data on dopaminergic/GABAergic juxtaglomerular neurons reported by Kiyokage and coworkers (2010), and serves as an additional proof that ARO immunopositive juxtaglomerular cells are dopaminergic.

To examine the relationship of ARO with proteins involved in the regulation of local intracellular calcium concentrations in the GL of the MOB, namely CR and CB, the calcium binding proteins characteristic of type II periglomerular cells (Kosaka et al. 1998), further double labeling studies were performed. First we examined if ARO colocalizes with either CR or CB. The same ARO immunoreactivity pattern was observed as in previous experiments, highlighting small somata with fine processes that either enter glomeruli or pass along, delineating glomerular borders. As for the calcium binding proteins, a large number of CR immunolabeled periglomerular cells were detected with numerous fine dendritic processes entering the glomeruli. The CB immunoreactive cells observed were less numerous and they also sent their dendrites into the glomeruli. Analyzing the immunoreactivity patterns with confocal microscopy, a complete separation was found between ARO immunolabeled neurons and CR or CB expressing periglomerular cells. Neurons containing calcium binding proteins always had smaller somata than ARO immunolabeled cells, they were often localized in the close vicinity of ARO expressing neurons, but no colocalization of ARO and CR or CB was detected in either section of the MOB of either animal studied (Fig. 4g, h, i, j, k, l).

Another protein which also plays a role in modulating intracellular calcium concentration and is expressed at high levels in the GL of the MOB is mGluR1 (Sahara et al. 2001, Dong et al. 2007). Moreover, dopaminergic periglomerular neurons are reported to express mGluR1 (Jian et al. 2010). Thus, TH and mGluR1 double immunolabeling experiments were performed to examine their colocalization in our material. In accordance with data reported in the literature, strong mGluR1 immunoreactivity was observed on the cellular membranes of every dopaminergic neuron and on other juxtaglomerular cells as well. The mGluR1 signal was not as homogeneous as the TH label, it appeared as a large number of dots present on neuronal membranes (Fig. 4m, n, o).

Neurochemical characterization of ERβ expressing cells in the GL

In our third series of experiments fluorescence double immunostainings were carried out and analyzed with confocal microscopy to examine the neurochemical properties of ERβ expressing cells in the GL of the MOB. As it was seen earlier with single immunolabeling, ERβ expression was more widespread than ARO immunostaining. ERβ was detected in most, if not all, periglomerular neurons and in astrocytes as well. We found a "speckled" pattern of ERβ immunolabel in the nuclei of dopaminergic neurons, GAD67 expressing neurons, CR and CB containing neurons, and in GFAP labeled astrocytes. The TH, GAD67, CR and CB immunolabels showed the same pattern and distribution as in the second series of experiments. The GFAP labeling filled evenly somata and cellular processes (Fig. 5).

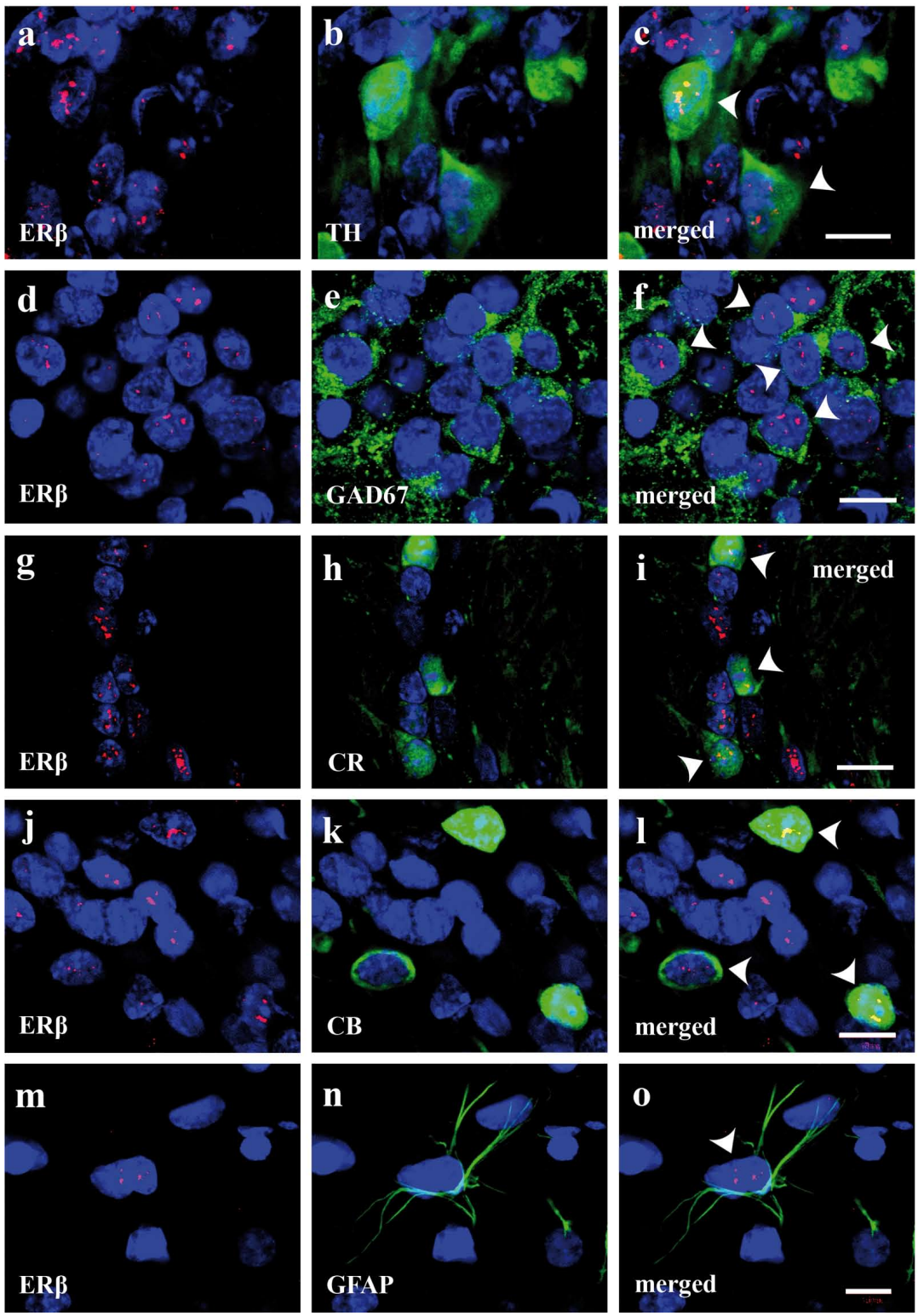

Fig. 5. Confocal single slice images of double immunofluorescences in the GL of the MOB to analyse the colocalization of ERβ with TH (a–c), GAD67 (d–f), CR (g–i), CB (j–l) and GFAP (m–o). ERβ signal is seen in red, while all other immunolabel is displayed in green. All sections were counterstained with DAPI. Overlays of images show that ERβ is expressed in TH+ (c), GAD67+ (f), CR+ (i), CB+ (l) neurons and in GFAP+ astrocytes (o) too. Arrowheads point to cells displaying colocalization. Scale bars are 10 μm.

DISCUSSION

Our results provide a solid immunohistochemical evidence of a novel feature of olfactory TH/GAD67 immunoreactive juxtaglomerular cells: they express ARO and, at the same time, they express ERβ, too. These cells are reported to participate in oligoglomerular and polyglomerular networks and their activity is a key factor in shaping interglomerular inhibition (Kiyokage et al. 2010). The ARO and ERβ expression of these cells is particularly intriguing in terms of olfactory information processing, since the basic activity pattern of OB projection neurons is formed by intraglomerular circuits, while the sharpening of mitral/tufted cell response pattern is achived *via* interglomerular inhibition (Wachowiak and Shipley 2006, Kiyokage et al. 2010). The ARO expression in the TH/GAD67 immunoreactive interneurons in the GL of the MOB raises the possibility of local estradiol synthesis. Moreover, the expression of ERβ in the same cells suggests that these cells are able to not only produce estradiol, but they can respond to it, too.

ARO expression was also observed in mitral cells, the principal output neurons, although, to a lesser extent. The ERβ expression was also present in the projection neurons, suggesting that the same estradiol production and response mechanism may work in both the output neurons and in the dopaminergic/GABAeric juxtaglomerular cells, which are in a strategic position in gating the flow of olfactory information to mitral cells (Shipley and Ennis 1996).

The amount of estrogens synthesized by ARO expressed in the OB is expected to depend on ARO activity. The activity of ARO is reversibly downregulated within minutes by increased concentration of intracellular calcium due to glutamaterg inputs in quail hypothalamic explants (Balthazart et al. 2006). In accordance with data reported in the literature, our results show that dopaminergic/GABAergic juxtaglomerular neurons express mGluR1 on their cellular membrane (Sahara et al. 2001) through which calcium may enter these cells upon direct or indirect input from the olfactory nerve (Kiyokage et al. 2010). Furthermore, no colocalization between TH and CB or TH and CR was detected in our experiments, suggesting that an increase in intracellular calcium concentration evoked by mGluR1 activation in these cells is not buffered either by CB or CR. Thus, it can be hypothesized that besides leading to a depolarization, the released calcium might also downregulate ARO enzymatic activity in the rat OB too.

Concerning ERβ expression, our double labeling immunofluorescence experiments showed that ERβ, in contrast to ARO, is expressed in a wide range of cell types, including even astrocytes. Moreover, ERβ was shown not only in cellular nuclei, but also on cellular processes in the EPL and on processes entering glomeruli. Consequently, estradiol in the OB may have a long term genomic role acting on nuclear receptors, and it may have a rapid, neurotransmitter-like effect acting on membrane receptors. The long term estradiol action in the OB may include modulation of astroglial reactions (Hoyk et al. 2004, Garcia-Ovejero et al. 2005) formation of sexual dimorphism of olfactory pathways during development (Horvath and Wikler 1999), neurogenesis throughout life (Brock et al. 2010, Veyrac and Bakker 2011), processing of olfactory cues guiding social and reproductive behavior (Pierman et al. 2008, Sorwell et al. 2008, Maruska and Fernald 2010) and olfactory memory formation (Sanchez-Andrade and Kendrick 2009).

On the other hand, the presence of ERβ on cellular processes suggests that 17β-estradiol may also participate in the rapid modulation of synaptic processing of olfactory information. There is evidence of fast changes in local estradiol concentration in the visual system in mice and in the avian auditory system regulated by visual and auditory inputs, respectively (Jeong et al. 2011a, b, Remage-Healey et al. 2011). As far as the olfactory system is concerned, at present there are no data on olfactory input driven fast changes of estrogen concentrations, but taking together the results of our present colocalization studies, a sensory input dependent ARO activity regulation can be hypothesized in the olfactory system too, resulting in rapid fluctuations of local estradiol levels.

CONCLUSIONS

The present report provides morphological evidence on a novel feature of the neurochemical character of dopaminergic/GABAergic juxtaglomerular neurons and principal output neurons of the MOB: they express ARO and ERβ, therefore they are capable to produce estrogens and respond to it. Moreover, the dopaminergic/GABAergic juxtaglomerular neurons of the GL in the MOB are capable to produce estrogens probably in an olfactory input dependent way *via* mGluR1 signaling, suggesting that estrogen circuits may participate in sharpening the mitral/tufted cell response pattern. It is perfectly in line with the

hypothesis that the sensory-neuroendocrine interaction is a general property of information processing in sensory systems (Jeong et al. 2011a).

ACKNOWLEDGEMENTS

This work was supported by the Hungarian National Office for Research and Technology (GVOP-3.2.1. 2004-04-0052/3.0, OM-00103/2008 GLINOLID, TÁMOP-4.2.2/08/1/2008-0002, TÁMOP-4.2.2/B-10/1-2010-0012 and TÁMOP-4.2.2.A-11/1/KONV-2012-0052), OTKA K075954, TeT ES-5/2008 and Bolyai Fellowship (E. Cs.). The authors wish to thank Dr. María Ángeles Arevalo for the CR antibody and Dr. Luis Miguel Garcia-Segura for the ARO antibody which served to test the specificity of the Santa Cruz ARO antibody.

REFERENCES

Abrous DN, Koehl M, LeMoal M (2005) Adult neurogenesis: from precursors to network and physiology. Physiol Rev 85: 523–569.

Azcoitia I, Yague JG, Garcia-Segura LM (2011a) Estradiol synthesis within the human brain. Neuroscience 191: 139–147.

Azcoitia I, Arevalo MA, De Nicola AF, Garcia-Segura LM (2011b) Neuroprotective actions of estradiol revisited. Trends Endocrinol Metab 22: 467–473.

Bakker J, Honda S, Harada N, Balthazart J (2004) Restoration of male sexual behavior by adult exogenous estrogens in male aromatase knockout mice. Horm Behav 46: 1–10.

Balthazart J, Baillien M, Ball GF (2006) Rapid control of brain aromatase activity by glutamatergic inputs. Endocrinology 147: 359–366.

Brock O, Keller M, Veyrac A, Douhard Q, Bakker J (2010) Short term treatment with estradiol decreases the rate of newly generated cells in the subventricular zone and main olfactory bulb of adult female mice. Neuroscience 166: 368–376.

Crespo C, Gracia-Llanes FJ, Blasco-Ibáñez JM, Gutièrrez-Mecinas M, Marqués-Marí AI, Martínez-Guijarro FJ (2003) Nitric oxide synthase containing periglomerular cells are GABAergic in the rat olfactory bulb. Neurosci Lett 349: 151–154.

Dong HW, Hayar A, Ennis M (2007) Activation of group I metabotropic glutamate receptors on main olfactory bulb granule cells and periglomerular cells enhances synaptic inhibition of mitral cells. J Neurosci 27: 5654–5663.

Fester L, Prange-Kiel J, Jarry H, Rune GM (2011) Estrogen synthesis in the hippocampus. Cell Tissue Res 345: 285–294.

Flores F, Naftolin F, Ryan KJ, White RJ (1973) Estrogen formation by the isolated perfused rhesus monkey brain. Science 180: 1074–1075.

Foidart A, Harada N, Balthazart J (1995) Aromatase-immunoreactive cells are present in mouse brain areas that are known to express high levels of aromatase activity. Cell Tissue Res 280: 561–574.

Garcia-Ovejero D, Azcoitia I, Doncarlos LL, Melcangi RC, Garcia-Segura LM (2005) Glia-neuron crosstalk in the neuroprotective mechanisms of sex steroid hormones. Brain Res Brain Res Rev 48: 273–286.

Garcia-Segura LM, Wozniak A, Azcoitia I, Rodriguez JR, Hutchison RE, Hutchison JB (1999) Aromatase expression by astrocytes after brain injury: implications for local estrogen formation in brain repair. Neuroscience 89: 567–578.

Garcia-Segura LM (2008) Aromatase in the brain: not just for reproduction anymore. J Neuroendocrinol 20: 705–712.

González A, Piferrer F (2003) Aromatase activity in the European sea bass (Dicentrarchus labrax L.) brain. Distribution and changes in relation to age, sex, and the annual reproductive cycle. Gen Comp Endocrinol 132: 223–230.

Guo XZ, Su JD, Sun QW, Jiao BH (2001) Expression of estrogen receptor (ER) -alpha and -beta transcripts in the neonatal and adult rat cerebral cortex, cerebellum, and olfactory bulb. Cell Res 11: 321–324.

Hojo Y, Hattori TA, Enami T, Furukawa A, Suzuki K, Ishii HT, Mukai H, Morrison JH, Janssen WG, Kominami S, Harada N, Kimoto T, Kawato S (2004) Adult male rat hippocampus synthesizes estradiol from pregnenolone by cytochromes P45017alpha and P450 aromatase localized in neurons. Proc Natl Acad Sci U S A 101: 856–870.

Horvath TL, Wikler KC (1999) Aromatase in developing sensory systems of the rat brain. J Neuroendocrinol 11: 77–84.

Hoyk Z, Párducz A, Garcia-Segura LM, (2004) Dehydroepiandrosterone regulates astroglia reaction to denervation of olfactory glomeruli. Glia 48: 207–216.

Hsu SM, Raine L, Fanger H (1981) The use of antiavidin antibody and avidin-biotin-peroxidase complex in immunoperoxidase technics. Am J Clin Pathol 75: 816–821.

Jakab RL, Horvath TL, Leranth C, Harada N, Naftolin F (1993) Aromatase immunoreactivity in the rat brain: gonadectomy-sensitive hypothalamic neurons and an

unresponsive "limbic ring" of the lateral septum-bed nucleus-amygdala complex. J Steroid Biochem Mol Biol 44: 481–498.

Jeong JK, Tremere LA, Burrows K, Majewska AK, Pinaud R (2011a) The mouse primary visual cortex is a site of production and sensitivity to estrogens. PLoS ONE 6: e20400.

Jeong JK, Burrows K, Tremere LA, Pinaud R (2011b) Neurochemical organization and experience-dependent activation of estrogen-associated circuits in the songbird auditory forebrain. Eur J Neurosci 34: 283–291.

Jian K, Cifelli P, Pignatelli A, Frigato E, Belluzzi O (2010) Metabotropic glutamate receptors 1 and 5 differentially regulate bulbar dopaminergic cell function. Brain Res 1354: 47–63.

Karahan S, Yarim M, Harada N (2008) Cytochrome P450 aromatase expression in canine nervous tissue: an immunohistochemical study. Pol J Vet Sci 11: 347–352.

Kiyokage E, Pan YZ, Shao Z, Kobayashi K, Szabo G, Yanagawa Y, Obata K, Okano H, Toida K, Puche AC, Shipley MT (2010) Molecular identity of periglomerular and short axon cells. J Neurosci 30: 1185–1196.

Kosaka K, Aika Y, Toida K, Heizmann CW, Hunziker W, Jacobowitz DM, Nagatsu I, Streit P, Visser TJ, Kosaka T (1995) Chemically defined neuron groups and their subpopulations in the glomerular layer of the rat main olfactory bulb. Neurosci Res 23: 73–88.

Kosaka K, Toida K, Margolis FL, Kosaka T (1997) Chemically defined neuron groups and their subpopulations in the glomerular layer of the rat main olfactory bulb--II. Prominent differences in the intraglomerular dendritic arborization and their relationship to olfactory nerve terminals. Neuroscience 76: 775–786.

Kosaka K, Toida K, Aika Y, Kosaka T (1998) How simple is the organization of the olfactory glomerulus?: the heterogeneity of so-called periglomerular cells. Neurosci Res 30: 101–110.

Kosaka K, Kosaka T (2005) Synaptic organization of the glomerulus in the main olfactory bulb: compartments of the glomerulus and heterogeneity of the periglomerular cells. Anat Sci Int 80: 80–90.

Kosaka T, Kosaka K (2008) Tyrosine hydroxylase-positive GABAergic juxtaglomerular neurons are the main source of the interglomerular connections in the mouse main olfactory bulb. Neurosci Res 60: 349–354.

Kosaka T, Kosaka K (2011) "Interneurons" in the olfactory bulb revisited. Neurosci Res 69: 93–99.

Krohmer RW, Boyle MH, Lutterschmidt DI, Mason RT (2010) Seasonal aromatase activity in the brain of the male red-sided garter snake. Horm Behav 58: 485–492.

Lephart ED (1996) A review of brain aromatase cytochrome P450. Brain Res Brain Res Rev 22: 1–26.

MacLusky NJ, Walters MJ, Clark AS, Toran-Allerand CD (1994) Aromatase in the cerebral cortex, hippocampus, and mid-brain: ontogeny and developmental implications. Mol Cell Neurosci 5: 691–698.

Maruska KP, Fernald RD (2010) Reproductive status regulates expression of sex steroid and GnRH receptors in the olfactory bulb. Behav Brain Res 213: 208–217.

Mirzatoni A, Spence RD, Naranjo KC, Saldanha CJ, Schlinger BA (2010) Injury-induced regulation of steroidogenic gene expression in the cerebellum. J Neurotrauma 27: 1875–1882.

Mitra SW, Hoskin E, Yudkovitz J, Pear L, Wilkinson HA, Hayashi S, Pfaff DW, Ogawa S, Rohrer SP, Schaeffer JM, McEwen BS, Alves SE (2003) Immunolocalization of estrogen receptor beta in the mouse brain: comparison with estrogen receptor alpha. Endocrinology 144: 2055–2067.

Naftolin F, Ryan KJ, Petro Z (1971) Aromatization of androstenedione by limbic system tissue from human foetuses. J Endocrinol 51: 795–796.

Naftolin F, Horvath TL, Jakab RL, Leranth C, Harada N, Balthazart J (1996) Aromatase immunoreactivity in axon terminals of the vertebrate brain. An immunocytochemical study on quail, rat, monkey and human tissues. Neuroendocrinology 63: 149–155.

Ou SK, Hwang M, Patterson PH (1993) A modified method for obtaining large amounts of high titer polyclonal ascites fluid. J Immunol Methods 165: 75–80.

Parrish-Aungst S, Shipley MT, Erdelyi F, Szabo G, Puche AC (2007) Quantitative analysis of neuronal diversity in the mouse olfactory bulb. J Comp Neurol 501: 825–836.

Pierman S, Douhard Q, Bakker J (2008) Evidence for a role of early oestrogens in the central processing of sexually relevant olfactory cues in female mice. Eur J Neurosci 27: 423–431.

Remage-Healey L, Dong S, Maidment NT, Schlinger BA (2011) Presynaptic control of rapid estrogen fluctuations in the songbird auditory forebrain. J Neurosci 31: 10034–10038.

Roselli CE, Horton LE, Resko JA (1985) Distribution and regulation of aromatase activity in the rat hypothalamus and limbic system. Endocrinology 117: 2471–2477.

Roselli CE, Liu M, Hurn PD (2009) Brain aromatization: classic roles and new perspectives. Semin Reprod Med 27: 207–217.

Sahara Y, Kubota T, Ichikawa M (2001) Cellular localization of metabotropic glutamate receptors mGluR1, 2/3, 5 and 7 in the main and accessory olfactory bulb of the rat. Neurosci Lett 312: 59–62.

Sanchez-Andrade G, Kendrick KM (2009) The main olfactory system and social learning in mammals. Behav Brain Res 200: 323–335.

Sanghera MK, Simpson ER, McPhaul MJ, Kozlowski G, Conley AJ Lephart ED (1991) Immunocytochemical distribution of aromatase cytochrome P450 in the rat brain using peptide-generated polyclonal antibodies. Endocrinology 129: 2834–2844.

Shinoda K, Yagi H, Osawa Y, Shiotani Y (1990) Involvement of specific placental antigen X-P2 in rat olfaction: an immunohistochemical study in the olfactory bulb. J Comp Neurol 294: 340–344.

Shinoda K, Nagano M, Osawa Y (1994) Neuronal aromatase expression in preoptic strial, and amygdaloid regions during late prenatal and early postnatal development in the rat. J Comp Neurol 343: 113–129.

Shipley MT, Ennis M (1996) Functional organization of olfactory system. J Neurobiol 30: 123–176.

Shughrue PJ, Lane MV, Merchenthaler I (1997) Comparative distribution of estrogen receptor-alpha and -beta mRNA in the rat central nervous system. J Comp Neurol 388: 507–525.

Sorwell KG, Wesson DW, Baum MJ (2008) Sexually dimorphic enhancement by estradiol of male urinary odor detection thresholds in mice. Behav Neurosci 122: 788–793.

Stoffel-Wagner B (2001) Neurosteroid metabolism in the human brain. Eur J Endocrinol 145: 669–679.

Toida K, Kosaka K, Aika Y, Kosaka T (2000) Chemically defined neuron groups and their subpopulations in the glomerular layer of the rat main olfactory bulb-IV. Intraglomerular synapses of tyrosine hydroxylase-immunoreactive neurons. Neuroscience 101: 11–17.

Veyrac A, Bakker J (2011) Postnatal and adult exposure to estradiol differentially influences adult neurogenesis in the main and accessory olfactory bulb of female mice. FASEB J 25: 1048–1057.

Wachowiak M, Shipley MT (2006) Coding and synaptic processing of sensory information in the glomerular layer of the olfactory bulb. Semin Cell Dev Biol 17: 411–423.

Yague JG, Muñoz A, de Monasterio-Schrader P, Defelipe J, Garcia-Segura LM, Azcoitia I (2006) Aromatase expression in the human temporal cortex. Neuroscience 138: 389–401.

Yague JG, Wang AC, Janssen WG, Hof PR, Garcia-Segura LM, Azcoitia I, Morrison JH (2008) Aromatase distribution in the monkey temporal neocortex and hippocampus. Brain Res 1209: 115–127.

Yague JG, Azcoitia I, DeFelipe J, Garcia-Segura LM, Muñoz A (2010) Aromatase expression in the normal and epileptic human hippocampus. Brain Res 1315: 41–52.